I. PRESENT APPROACH RELATED TO THE KOHN-SHAM METHODS

In section IIA. of Ref. [1], Kohn and Sham defined a noninteracting system (NIS) described by a local potential. The kinetic energy of this NIS was termed T_s. Then, the energy E of the fully interacting system (FIS) was written as:

$$E = \underbrace{T_s + V_{ne} + J}_{accurate} + \underbrace{E_{xc}}_{approx.} \tag{1}$$

where V_{ne} and J arise from the nucleus-electron and coulombic interactions respectively, and E_{xc} stands for the *exchange-correlation* contribution. In connexion with the present approach it is worthwhile empasizing that the purpose of eq. (1) was to separate two components: the sum $T_s + V_{ne} + J$ to be evaluated accurately, and E_{xc} to be given by a density functional.

In section IIB. of Ref. [1], by contrast the NIS was subjected to a nonlocal Hartree-Fock like potential. The kinetic energy of this second NIS was again named T_s for the sake of simplicity. From this new definition of T_s the following expression for the energy E came out in replacement of eq. (1):

$$E = \underbrace{T_s + V_{ne} + J + K}_{accurate} + \underbrace{E_c}_{approx.}, \tag{2}$$

where the exchange component K was extracted from the wave function of the NIS, as well as T_s, V_{ne} and J. Then, only the *correlation* term E_c defined by (2) was derived from the density. At the beginning this slightly more expensive variant was less followed than the previous one. As a major argument in favor of the first scheme, it was found that the shape of the exchange correlation hole displayed favorable error cancellations between its exchange and correlation parts[2–5]. Nevertheless, more recently interest for the second scheme was restarted by the success of hybrid functionals, and by functionals including "exact exchange" (see e.g. Refs. [6–14]). Further supporting that direction, E_c is typically one order of magnitude smaller as E_{xc}. Therefore the error on E_c is also expected to be smaller than the error on E_{xc}.

For the present purpose the ground state energy is decomposed as follows:

$$E = \underbrace{T_s + V_{ne} + J + K + E_{cw}}_{accurate} + \underbrace{E_{cd}}_{approx.} . \tag{3}$$

T_s refers to the kinetic energy of an unspecified NIS, and E_{cw} and E_{cd} are fractions of the correlation energy. By comparison with the previous two variants, in eq. (3) $T_s+V_{ne}+J+K$ is obtained from a non interacting wave function whereas E_{cw} arise from a partially interacting wave function. Finally, E_{cd} is entirely provided by a density functional. The motivation for partition (3) will be discussed in the next section. The arguments stem from an analysis of the correlation energy in terms of wave function.

II. ARBITRARINESS IN THE DEFINITION OF THE CORRELATION ENERGY

For accessing the ground state energy E the usual procedure in quantum chemistry is to define, as a first step, a model system which can be calculated easily. An independent particle model in an effective field is often used for that purpose. Then, the energy of the model, denoted as E_m, typically yields about 99% of the total electronic energy. As a second step the effort of the calculation is focused on the residue, E_r, defined such that

$$E = E_m + E_r. \tag{4}$$

That residue, which is responsible for only 1% of the total energy often accounts, yet, for the chemistry of the system. Hence it is of prime importance to define E_r so that further approximations reveal efficient. Several definitions might be considered for E_r. The simplest model for that purpose is probably the Hartree product. In that case, E_r corresponds to the "correlation energy" between electrons, in a statistical sense. In quantum chemistry the model is traditionnaly chosen to satisfy the restricted Hartree-Fock equations[15], and E_r is again refered to as the correlation energy (even though in that case parallel spins are correlated in a statistical sense). Going one step further spin-unrestricted models could be used as well (especially for open-shells)[16], or even models described by an arbitrary number of determinants[17]. As a rule, the more the model ressembles the true system, the more accurate and expensive the computation of E_r. Within density functional theory the Kohn-Sham model provides an alternative definition of E_r (see e.g. [18, 19]). In that case E_r can be evaluated easily, but with uncontroled errors. Close to that line, models

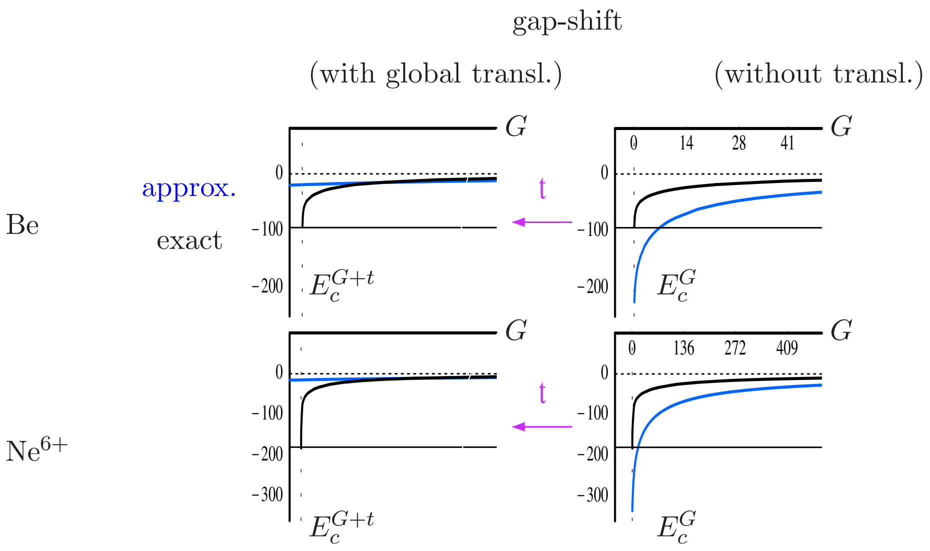

FIG. 1: Be (first line), Ne^{6+} (second line). Gap-shift variant (right), gap-shift plus global translation t variant (left). Exact ρ part of the coupling (black), approximate ρ part of the coupling (grey, or blue in the colored version), in mHartree, depending on G, in Hartree. $G(\kappa)$ is related to κ in eq. (26) of the paper.

not requiring the knowledge of the density[20, 21] are an even more convenient option, from a practical point of view. Accordingly, we propose in the present to take as a model the Krieger, Li and Iafrate (KLI)[11] NIS. Then, we will separate the residual energy into two components, E_{cw} and E_{cd}, one being evaluated with a wave function and the other with a density functional.The purpose in this further decomposition is to extract from E_r only those correlating effects that are badly described by density functionals, and handle them more accurately with a wave function. In the same time, the density functional scheme for the remaining part of E_r is expected to be more efficient than when used for both E_{cw} and E_{cd}. In that way we aim at better controling the density functional errors. The prescriptions to achieve such a separation between E_{cw} and E_{cd} are discussed in next section, based on an analysis of E_c in terms of the wave function.

III. CYLINDRICAL COORDINATES FOR EVALUATING THE INTEGRALS

The evaluation of the integrals for the gap-shift (eqs. (A5) and (A6) in the paper) and the cutoff (eqs. (B4), (B5) and (B6) in the paper) variants was performed with the cylindrical coordinates (x, ρ, φ) introduced by Heisenberg[22] and used by Macke[23]. For the cutoff variant, the integration domain was detailed in the following, by taking into account the

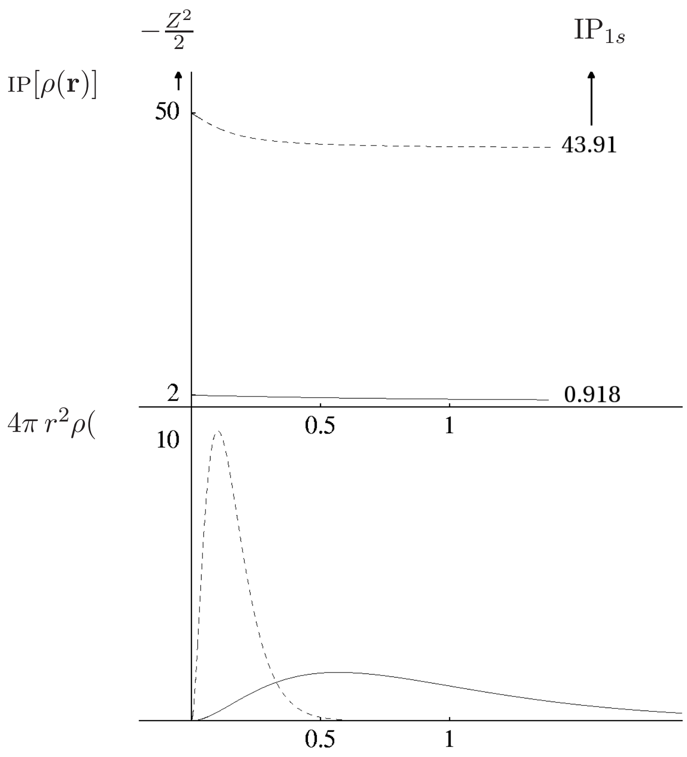

FIG. 2: $Z = 2$ (plain line) and $Z = 10$ (dotted line) in the He series. IP$[\rho(\mathbf{r})] = 1/8|\nabla\rho(r)/\rho(r)|^2$ (top), and radial density probability $4\pi\, r^2\rho(r)$ (bottom) as functions of r (a.u.). The ionisation potential (as estimated from KLI orbital energies) of shell 1s (IP$_{1s}$) has been superimposed with the upper curve.

additional constraint that the unoccupied momenta $\mathbf{k}+\mathbf{q}$ be lower than κ. Thus, the integral

$$\begin{aligned} &\int d\mathbf{k}\, \theta(\mathbf{k},\mathbf{q})\, \theta(\kappa - |\mathbf{k}+\mathbf{q}|) \\ = &\int d\mathbf{k}\, \theta(1-k)\theta(|\mathbf{k}+\mathbf{q}|-1)\theta(\kappa - |\mathbf{k}+\mathbf{q}|), \end{aligned} \tag{5}$$

was separated according to the norm of the transfer momenta $\mathbf{q}$ and the cutoff κ. Three regions were distinguished (cf. Figs. 6, 7 and 8 respectively for a graphical representation):

- $q < 2 \quad \text{and} \quad \kappa > \sqrt{2-(q-1)^2}$,
- $q < 2 \quad \text{and} \quad \kappa \le \sqrt{2-(q-1)^2}$,
- $q > 2 \quad \text{and} \quad \kappa > q - 1$.

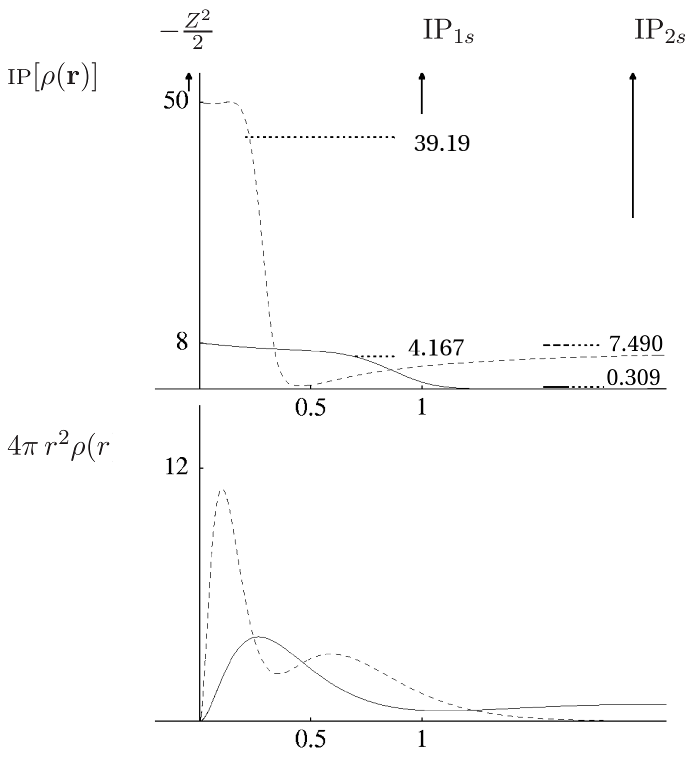

FIG. 3: $Z = 4$ (plain line) and $Z = 10$ (dotted line) in the Be series. IP$[\rho(\mathbf{r})] = 1/8|\nabla\rho(r)/\rho(r)|^2$ (top), and radial density probability $4\pi\, r^2\rho(r)$ (bottom) as functions of r (a.u.). The ionisation potentials (as estimated from KLI orbital energies) of shells 1s (IP$_{1s}$) and 2s (IP$_{2s}$) have been superimposed with the upper curve.

In these figures, m et n are the distances

$$m = \frac{1-(\kappa-q)^2}{2q}; \quad n = \frac{\sqrt{2\kappa^2(q^2+1)-(q^2-1)^2-\kappa^4}}{2q}. \tag{6}$$

and min is the function giving the minimum of two arguments.

IV. ASYMPTOTIC BEHAVIOUR OF THE DENSITY FUNCTIONAL FOR THE FICTITIOUS SYSTEM WITH CUTOFF κ AT LARGE κ

In first place, let us consider the RPA* approximation of the correlation energy. We are interested in the large-κ behaviour of the difference $\epsilon_c^{\text{RPA}^\star} - \epsilon_c^{\text{RPA}^\star,\kappa} =\propto \int_0^\infty dq\, \bar{S}_2^{\text{RPA}^\star}(\text{q}) - \int_0^\infty dq\, \bar{S}_2^{\text{RPA}^\star,\kappa}(\text{q})$. As soon as the two Fermi spheres are located inside the cutoff (i.e. $q < \kappa - 1$), there is no difference between $\bar{S}_2^{\text{RPA}^\star}(\text{q})$ and $\bar{S}_2^{\text{RPA}^\star,\kappa}(\text{q})$. Moreover, for $q > \kappa + 1$ (i.e.

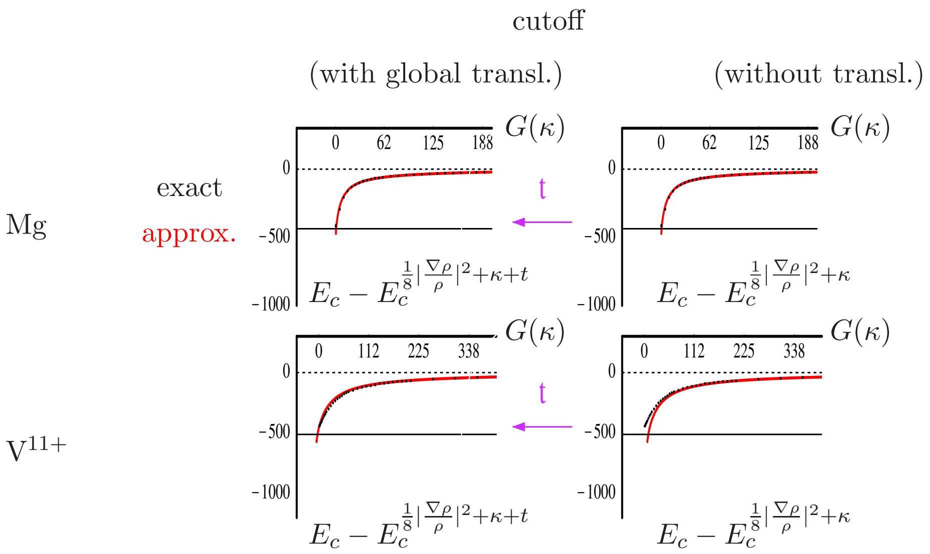

FIG. 4: Mg (first line), V^{11+} (second line). Local cutoff $\frac{1}{8}|\frac{\nabla\rho}{\rho}|^2$ variant (right), local cutoff plus global translation t variant (left). Exact ρ part of the coupling (black), approximate ρ part of the coupling (grey, or red in the colored version), in mHartree, depending on G, in Hartree. $G(\kappa)$ is related to κ in eq. (26) of the paper.

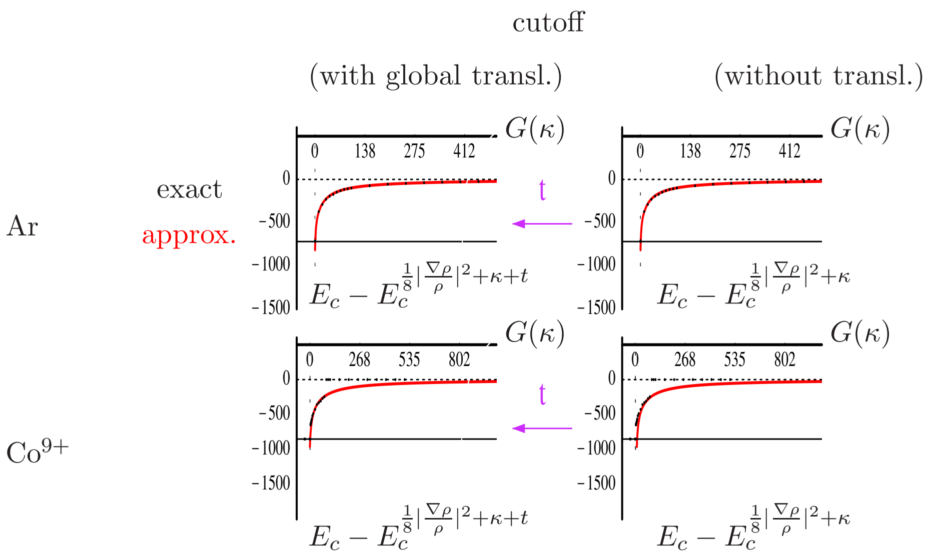

FIG. 5: Ar (first line), Co^{9+} (second line). Local cutoff $\frac{1}{8}|\frac{\nabla\rho}{\rho}|^2$ variant (right), local cutoff plus global translation t variant (left). Exact ρ part of the coupling (black), approximate ρ part of the coupling (grey, or red in the colored version), in mHartree, depending on G, in Hartree. $G(\kappa)$ is related to κ in eq. (26) of the paper.

when the cutoff does not intersect the second Fermi sphere), $\bar{S}_2^{\mathrm{RPA}^\star,\kappa}(\mathrm{q})$ does not contribute

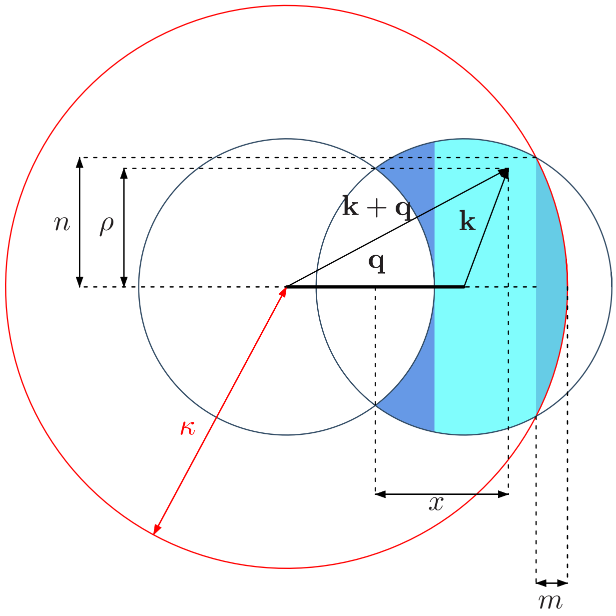

$q < 2; \quad \kappa > \sqrt{2-(q-1)^2}$

FIG. 6: Integration domains for the electron gas with cutoff, in cylindrical coordinates (from left to right): $\int_0^{1-\frac{q}{2}} dx \int_{\sqrt{1-(x+\frac{q}{2})^2}}^{\sqrt{1-(x-\frac{q}{2})^2}} \rho\, d\rho \int_0^{2\pi} d\varphi$ (dark), $\int_{1-\frac{q}{2}}^{\min(\frac{q}{2}+1,\kappa-\frac{q}{2}-m)} dx \int_0^{\sqrt{1-(x-\frac{q}{2})^2}} \rho\, d\rho \int_0^{2\pi} d\varphi$ (light), $\int_{\min(\frac{q}{2}+1,\kappa-\frac{q}{2}-m)}^{\min \frac{q}{2}+1,\kappa-\frac{q}{2}} dx \int_0^{\sqrt{\kappa^2-(\frac{q}{2}+x)^2}} \rho\, d\rho \int_0^{2\pi} d\varphi$ (median).

to $\epsilon_c^{\mathrm{RPA}^\star,\kappa}$. The two remarks just above allow to make the following simplifications:

$$\epsilon_c^{\mathrm{RPA}^\star} - \epsilon_c^{\mathrm{RPA}^\star,\kappa} \propto \int_{\kappa-1}^{\infty} dq\, \bar{S}_2^{\mathrm{RPA}^\star}(\mathrm{q}) - \int_{\kappa-1}^{\kappa+1} dq\, \bar{S}_2^{\mathrm{RPA}^\star,\kappa}(\mathrm{q}). \tag{7}$$

As we are interested in the large κ limit of eq. (7), let us assume that $\kappa > 3$. Then for the integrands in eq. (7) only the case $q > 2$ needs be considered: $\bar{S}_2^{\mathrm{RPA}^\star}(\mathrm{q})$ is obtained by integration over the domains $\int_{\frac{q}{2}-1}^{\frac{q}{2}+1} dx \int_0^{\sqrt{1-(x-\frac{q}{2})^2}} \rho\, d\rho \int_0^{2\pi} d\phi$ (see Ref. [23] for instance), and $\bar{S}_2^{\mathrm{RPA}^\star,\kappa}(\mathrm{q})$ by integration over the domain $\int_{\kappa-1}^{\kappa+1} dq (\int_{\frac{q}{2}-1}^{\frac{\kappa^2-1}{2q}} dx \int_0^{\sqrt{1-(\frac{q}{2}-x)^2}} \rho\, d\rho + \int_{\frac{\kappa^2-1}{2q}}^{\kappa-\frac{q}{2}} dx \int_0^{\sqrt{\kappa^2-(\frac{q}{2}+x)^2}} \rho\, d\rho) \int_0^{2\pi} d\phi$ (cf. Fig. 8 for $\kappa > 3$). In equation (7), large-κ developments of the integrands can be performed after the change of variables $q \to q + \kappa$ has been made in the $[\kappa - 1, \kappa + 1]$ interval. We obtain

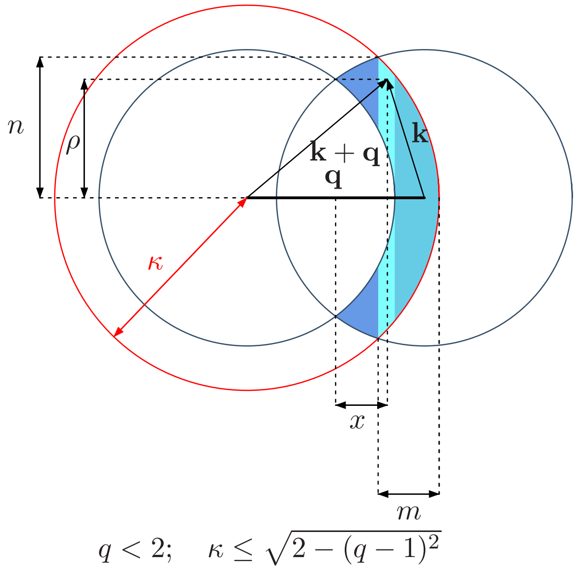

FIG. 7: Integration domains for the electron gas with cutoff, in cylindrical coordinates (from left to right): $\int_0^{\kappa-\frac{q}{2}-m} dx \int_{\sqrt{1-(x+\frac{q}{2})^2}}^{\sqrt{1-(x-\frac{q}{2})^2}} \rho\, d\rho \int_0^{2\pi} d\varphi$ (dark), $\int_{\kappa-\frac{q}{2}-m}^{1-\frac{q}{2}} dx \int_{\sqrt{1-(x+\frac{q}{2})^2}}^{\sqrt{\kappa^2-(x+\frac{q}{2})^2}} \rho\, d\rho \int_0^{2\pi} d\varphi$ (light), $\int_{1-\frac{q}{2}}^{\kappa-\frac{q}{2}} dx \int_0^{\sqrt{\kappa^2-(\frac{q}{2}+x)^2}} \rho\, d\rho \int_0^{2\pi} d\varphi$ (median).

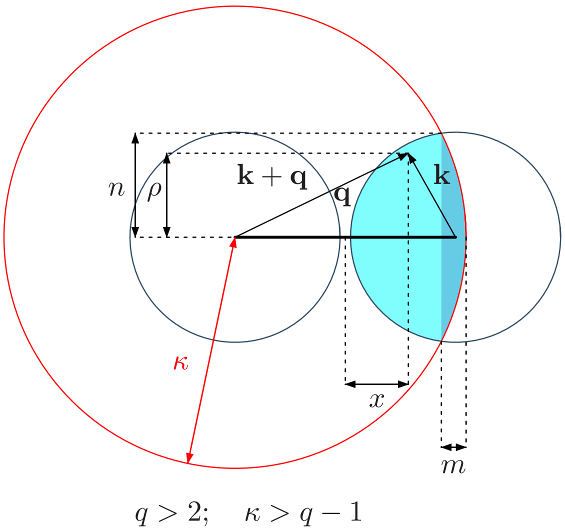

FIG. 8: Integration domains for the electron gas with cutoff, in cylindrical coordinates (from left to right): $\int_{\frac{q}{2}-1}^{\min(\frac{q}{2}+1,\frac{\kappa^2-1}{2q})} dx \int_0^{\sqrt{1-(x-\frac{q}{2})^2}} \rho\, d\rho \int_0^{2\pi} d\varphi$ (light), $\int_{\min(\frac{q}{2}+1,\kappa-\frac{q}{2}-m)}^{\min(\frac{q}{2}+1,\kappa-\frac{q}{2})} dx \int_0^{\sqrt{\kappa^2-(x+\frac{q}{2})^2}} \rho\, d\rho \int_0^{2\pi} d\varphi$ (median).

$$\begin{aligned}\epsilon_c^{\text{RPA}^\star} - \epsilon_c^{\text{RPA}^\star,\kappa} &= \int_{-1}^{1} dq\, \bar{S}_2^{\text{RPA}^\star}(\mathrm{q}+\kappa) + \int_{\kappa+1}^{\infty} dq\, \bar{S}_2^{\text{RPA}^\star}(\mathrm{q}) \\ &- \int_{-1}^{1} dq\, \bar{S}_2^{\text{RPA}^\star,\kappa}(\mathrm{q}+\kappa). \end{aligned} \tag{8}$$

Then the integration over q is performed yielding (in the same order)

$$\begin{aligned}\epsilon_c^{\text{RPA}^\star} - \epsilon_c^{\text{RPA}^\star,\kappa} \underset{\kappa\to\infty}{=} & \left[-\frac{16}{3\,\kappa^4\,\pi^2} + \mathcal{O}(\kappa^{-6})\right] \\ + & \left[-\frac{8}{9\,\kappa^3\,\pi^2} + \mathcal{O}(\kappa^{-4})\right] \\ - & \left[-\frac{208}{105\,\kappa^4\,\pi^2} + \mathcal{O}(\kappa^{-5})\right] \end{aligned} \tag{9}$$

Thus, the difference $\epsilon_c^{\text{RPA}^\star} - \epsilon_c^{\text{RPA}^\star,\kappa}$ starts with $-8/(9\,\kappa^3\,\pi^2)$ at large κ. Moreover, as $q_{ex} > q$ as $q > 2$, it is not expected that the inclusion of the exchange diagrams of the approximation RPA* + RPAEX*(1) will modify this behaviour. Another remark is that this result is independent of r_s (at small r_s), as with the gap-shift variant. It can be concluded that with the cutoff variant the correlation energy is obtained faster than with the gap-shift variant ($1/G \sim 2/(\kappa^2 - 1)$).

[1] W. Kohn and L. J. Sham, Phys. Rev. A **140**, 1133 (1965).

[2] V. Tschinke and T. Ziegler, Can. J. Chem. **67**, 460 (1989).

[3] V. Tschinke and T. Ziegler, J. Chem. Phys. **93**, 8051 (1990).

[4] R. van Leeuwen and E. J. Baerends, Phys. Rev. A **49**, 2421 (1994).

[5] O. Gritsenko, R. van Leeuwen, and E. J. Baerends, Int. J. Quantum Chem. **57**, 17 (1996).

[6] A. D. Becke, J. Chem. Phys. **98**, 1372 (1993).

[7] A. D. Becke, J. Chem. Phys. **98**, 5648 (1993).

[8] E. Engel and R. M. Dreizler, J. Comp. Chem. **20**, 31 (1999).

[9] E. Engel, A. Höck, and R. M. Dreizler, Phys. Rev. A **61**, 032502 (2000).

[10] E. Engel, A. Höck, and R. M. Dreizler, Phys. Rev. A **62**, 042502 (2000).

[11] J. B. Krieger, Y. Li, and G. J. Iafrate, *Recent developments in Kohn-Sham theory for orbital-dependant exchange-correlation energy functionals* (Plenum Press, New-York, 1995).

[12] A. Görling, Phys. Rev. Lett. **83**, 5459 (1999).

[13] F. D. Sala and A. Görling, J. Chem. Phys. **115**, 5718 (2001).

[14] M. Grüning, O. V. Gritsenko, and E. J. Baerends, J. Chem. Phys. **116**, 9591 (2002).

[15] P.-O. Löwdin, Adv. Chem. Phys. **2**, 207 (1959).

[16] P. C̀ársky and I. Hubac̀, Theor. Chim. Acta. **80**, 407 (1991).

[17] G. C. Lie and E. Clementi, J. Chem. Phys. **60**, 1274 (1974).

[18] A. Savin and H. Preuss, Theor. Chim. Acta **70**, 207 (1986).

[19] E. K. U. Gross, M. Petersilka, and T. Grabo, *Chemical Applications of Density Functional Theory* (B.B. Laird and R.B. Ross and T. Ziegler ed(s), Oxford, 1996).

[20] E. Engel and R. M. Dreizler, J. Comp. Chem. **20**, 31 (1999).

[21] C. Gutlé, J. L. Heully, J. B. Krieger, and A. Savin, Phys. Rev. A **66**, 012504 (2002).

[22] W. Heisenberg, Z. Naturforschg. **2a**, 185 (1947).

[23] W. Macke, Z. Naturforschg. **5a**, 192 (1950).